

## Strong Acidity of MFI-Type Ferrisilicate Determined by Temperature-Programmed Desorption of Ammonia

Naonobu Katada,\* Tetsuo Miyamoto, Hosne Ara Begum, Norihiro Naito, and Miki Niwa

Department of Materials Science, Faculty of Engineering, Tottori University, 4-101 Koyama-cho Minami, Tottori 680-8552, Japan

Akihiko Matsumoto and Kazuo Tsutsumi

Department of Materials Science, Faculty of Engineering, Toyohashi University of Technology, Tempaku-cho, Toyohashi, 441-8580, Japan

Received: December 13, 1999; In Final Form: March 27, 2000

Ammonia temperature-programmed desorption (TPD) with water vapor treatment method was applied to MFI-type ferrisilicate, and theoretical analysis was carried out to determine the acid amount and strength exactly. At the low iron content where isomorphous substitution of iron into the silicate matrix was predominant, a quite strong acid site with 150–180 kJ mol<sup>-1</sup> adsorption heat of ammonia, which was stronger than that on aluminosilicate, was observed. The determined acidic property was in good agreement with microcalorimetry. Therefore, it is concluded that the isomorphous substitution of iron into the MFI structure generates a stronger acid site than that by aluminum.

### Introduction

Since early studies<sup>1</sup> of ferrisilicate molecular sieve, it has been believed that isomorphous substitution of silicon by iron generates an acid site weaker than that by aluminum.<sup>2</sup> Frequency of O–H stretching<sup>1</sup> and its shift by adsorption of nitrogen, carbon monoxide,<sup>3</sup> ethene, and benzene<sup>4</sup> were smaller on the MFI ferrisilicate than those on aluminosilicate analogue (ZSM-5), suggesting a stronger O–H bond and weaker interaction with these bases. Temperature-programmed desorption (TPD) of ammonia on the ferrisilicate showed lower temperature of desorption peak maximum than that on aluminosilicate.<sup>1</sup> Many researchers have accepted the acid strength sequence B < Fe < Ga < Al in corresponding metasilicates because this order agrees well with the catalytic activity for a reaction that is believed to be a typical acid-catalyzed one such as cracking of alkane. The sequence of acid strength is interesting from the viewpoint of theoretical chemistry, and therefore quantum chemical calculations according to this sequence have been published.<sup>5–9</sup>

However, there appears some controversy. Careful measurements of calorimetry showed that the adsorption heat of ammonia was too similar to distinguish the acid strength of the MFI type ferri-, gallo-, and aluminosilicates.<sup>10</sup> Choudhary reported quite high catalytic activity of the ferrisilicate for liquid-phase Friedel–Crafts type alkylation of benzene with benzyl chloride,<sup>11</sup> which is usually catalyzed by solid superacid. These phenomena are possibly correlated with strong acidity of ferrisilicate. In the chemistry of clay minerals, iron-containing montmorillonite is known to possess stronger acidity than aluminum-containing analogue.<sup>12</sup>

Hence the early estimation of the acid strength becomes questionable. Because the acid strength is defined as the equilibrium constant with respect to the reaction between the

acid and a base such as ammonia and amine,<sup>13</sup> only a method using an ammonia (or amine) probe such as TPD and calorimetric measurement of adsorption heat can determine the absolute scale of acid strength. In other words, the IR technique and test reaction cannot determine the absolute acid strength. Especially the alkane cracking on the MFI silicates has complicated mechanisms, as discussed,<sup>14</sup> and is affected by the slow diffusion of the reactant and intermediates; the shape selectivity is evidence of the diffusion control, and therefore it is difficult to consider the activity for this reaction as a measure of acid strength. On the other hand, the conventional method of TPD of ammonia has two problems: unnecessary ammonia weakly held on nonacidic site,<sup>15</sup> e.g., hydrogen-bonded on ammonium cation,<sup>16</sup> confuses the TPD spectrum, and the readsorption of ammonia affects the peak maximum temperature.<sup>15</sup> We have pointed out that the difference of measurement conditions of TPD varies the peak maximum temperature widely in the range of some 10 K because of the latter problem.<sup>17</sup> Difference of the peak maximum temperature between ferri- and aluminosilicate is usually observed to be within 100 K,<sup>1,5,18–21</sup> and in some cases the observed peak has a too broad and complicated shape to exactly determine the peak maximum.<sup>5,18,20,22</sup> Moreover, most of these studies were based on measurements on only a few samples; hence the difference between the framework and extraframework species of iron seemed unclear. Therefore the conclusion obtained from the conventional measurements of the acidic property of ferrisilicate becomes doubtful.

It has been pointed out that the conventional ammonia TPD method is not useful because of the above-mentioned disadvantages.<sup>23,24</sup> We have improved the experimental and analytical methods in order to overcome them. First, the water vapor treatment technique was established to remove the unnecessary ammonia species based on the nature of the chemical bond between ammonia and solid,<sup>16</sup> based on the pioneering works

\* Corresponding author. E-mail: katada@chem.tottori-u.ac.jp.

by Bagnasco<sup>25</sup> and researchers of Mobil Oil.<sup>26</sup> Second, a method to calculate the adsorption heat of ammonia as a measure of acid strength from the peak area, position, and shape was proposed on the basis of the thermodynamics.<sup>17,27</sup> It should be noted that the proposed method does not ignore the readsorption of ammonia, and on this point it is different from the conventional energy calculation<sup>28,29</sup> from the TPD spectrum which assumes kinetic control. Already we have applied these methods to various zeolites<sup>16,27,30–32</sup> and nonzeolitic materials.<sup>33–35</sup> The investigation on the MFI-type gallosilicate changed the conventional interpretation of acidity on this material: it has been believed to have weaker acidity than aluminosilicate, but it was clarified that the isomorphous substitution of gallium in silicate generated the acid site quite similar in strength to that of aluminosilicate.<sup>36</sup> Here we report the investigation on the acidic property of the MFI-type ferrisilicate with various compositions by the developed techniques of ammonia TPD.

## Experimental Section

**Synthesis of Ferrisilicate.** Ferrisilicate was synthesized principally according to literature.<sup>2</sup> Iron nitrate and tetra-*n*-propylammonium bromide were solved into an aqueous solution, and this was dropped slowly into a Ludox HS40 silicate solution. Sodium carbonate solution was then added. Sodium hydroxide or sulfuric acid was added to adjust the pH to 9.7. The mixed solution was stirred and heated at 423 K for 72 h in an autoclave. The yielded solid was filtered, washed with water, and finally calcined at 813 K for 20 h in flowing oxygen. The thus obtained Na-type ferrisilicate was converted into H-type by ion exchange in an ammonium nitrate solution at 343 K for 24 h, followed by calcination in flowing oxygen at 813 K for 20 h. The iron and sodium contents were measured by an inductively coupled plasma (ICP) photoemission spectrometer (Shimadzu ICPS-5000). The contamination of aluminum was confirmed to be less than  $10^{-2}$  mol kg<sup>-1</sup>.

Impregnation of iron on ferrisilicate was carried out in order to clarify the acidic property of extraframework iron species. The ferrisilicate powder was put into an aqueous solution of iron(III) nitrate, heated on a hot plate, dried, and calcined at 813 K for 20 h in flowing oxygen. Iron oxide (BET surface area, 12 m<sup>2</sup> g<sup>-1</sup>) was also prepared as a comparison by hydrolysis of iron nitrate with ammonia followed by calcination at 773 K in air.

**Characterization.** To show the crystal structure, powder X-ray diffraction (XRD) was recorded by a Rigaku Miniflex Plus diffractometer with 0.45 kW Cu K $\alpha$  X-ray source (30 kV, 15 mA).

<sup>29</sup>Si NMR (nuclear magnetic resonance) was measured by a JEOL GSX 270 spectrometer with 53.67 MHz magnetic field frequency, 1.8  $\mu$ s of 40° pulse width, 15 s observation time and 10 kHz spinning rate. ESR (electron spin resonance) spectrum was collected by JEOL JES-FE2GX spectrometer with 0.08 g of the sample at 113 K.

Adsorption isotherm of nitrogen was measured at 77 K under 1 Pa to 90 kPa of the nitrogen pressure ( $P/P^\circ = 10^{-4}$ –0.9). The surface area was calculated from the isotherm according to the Langmuir equation.

A scanning electron microscopy (SEM) photograph was taken with a JEOL JSM-5800 scanning microscope after the deposition of thin gold film by a JEOL FINE COAT JFC-1100 ion sputter. The infrared (IR) spectrum was collected on the self-supporting disk with 10 mm diameter molded from 10–20 mg of silicate powder in an in situ cell by a JASCO FT/IR-5300 spectrometer.

**Temperature-Programmed Desorption of Ammonia.** The equipment [homemade or Japan Bel Inc. TPD-1-AT-(NH<sub>3</sub>)] and procedure were detailed in our review.<sup>31</sup> The sample (0.1 g) was set in a quartz cell and evacuated at 773 K for 1 h under <0.4 Pa of evacuation degree. Then ammonia (13.3 kPa) was introduced into the cell, and the pressure was kept for 30 min at 373 K. After evacuation for 30 min, water vapor was introduced into the sample cell; i.e., the sample was exposed to water vapor (2–4 kPa, vapor pressure at the room temperature) at 373 K for 30 min, followed by evacuation for 30 min. For the standard experiments, the introduction of water vapor and evacuation were repeated again. After these treatments, the adsorbed ammonia was desorbed in helium flow (0.044 mmol s<sup>-1</sup>) under ca. 13.3 kPa of total pressure with a 10 K min<sup>-1</sup> heating rate from 373 K. The desorbed ammonia was analyzed by a mass spectrometer (ULVAC UPM-ST-200 or ANELVA M-QA 100 F). Although the molecular weight of ammonia was 17, the fragment with  $m/e = 16$  was used to quantify ammonia, because the parent peak with  $m/e = 17$  was affected by the desorbed water.<sup>16</sup> After the measurement, a known amount of ammonia was fed to calibrate the mass spectrum intensity.

The obtained spectrum was analyzed with the curve-fitting method based on the assumption that equilibrium exists between the gaseous and adsorbed ammonia, and the readsorption of ammonia freely occurs.<sup>27</sup> The TPD spectrum was simulated according to the theoretical equation expressing the desorption of ammonia:

$$C_g = -\frac{\beta A_0 W}{F} \frac{d\theta}{dT} = \frac{\theta}{1-\theta} \frac{p^\circ}{RT} \exp\left(-\frac{\Delta H}{RT}\right) \exp\left(\frac{\Delta S}{R}\right) \quad (1)$$

where  $C_g$  is the concentration of ammonia in gas phase (mol m<sup>-3</sup>),  $\beta$  is the heating rate (K s<sup>-1</sup>),  $A_0$  is the desorption amount of ammonia (mol kg<sup>-1</sup>),  $W$  is the sample amount (kg),  $F$  is the flow rate of carrier gas (m<sup>3</sup> s<sup>-1</sup>),  $\theta$  is the coverage,  $p^\circ$  is the pressure of standard conditions ( $1.013 \times 10^5$  Pa),  $R$  is the gas constant (8.314 J K<sup>-1</sup> mol<sup>-1</sup>),  $T$  is the temperature (K),  $\Delta H$  is the enthalpy change (adsorption heat of ammonia, J mol<sup>-1</sup>), and  $\Delta S$  (J K<sup>-1</sup> mol<sup>-1</sup>) is the entropy change consisting of 95 J K<sup>-1</sup> mol<sup>-1</sup> of the constant term and the mixing term dependent on  $C_g$ . The parameters  $\Delta H_{\text{avg}}$ , the averaged value of  $\Delta H$ , and  $\sigma$ , distribution (standard deviation) of  $\Delta H$ , were adjusted to fit the simulated curve with the observed one. Thus the parameter set which gave the best fitted curve was selected, and this must show the acidic property of silicate.<sup>27</sup>

**Microcalorimetry.** Powder sample (1.2 g) was evacuated at 773 K for 5 h, and ammonia was introduced at 473 K. The adsorption heat was measured by the method described elsewhere.<sup>37</sup>

**Catalytic Cracking of *n*-Octane.** The sample (50 mg) was set in a Pyrex tube (4 mm i.d.) and pretreated at 773 K for 1 h in 30 cm<sup>3</sup> min<sup>-1</sup> flowing helium which was purified by passing through a liquid nitrogen trap. Subsequently 1 mm<sup>3</sup> of liquid *n*-octane (octane in IUPAC rule) was vaporized and fed into the catalyst bed at 673 K. The outlet was directly connected to a column of silicone SE-30, and the products were analyzed by a flame ionization detector (FID). All the experiments were carried out under differential conditions (conversion <2%). The cracking of isooctane (2,2,4-trimethylpentane in IUPAC) was carried out under the same conditions.

## Results

**Structure of Synthesized Ferrisilicate.** As shown in Figure 1, the XRD spectra indicated that all the samples had the MFI

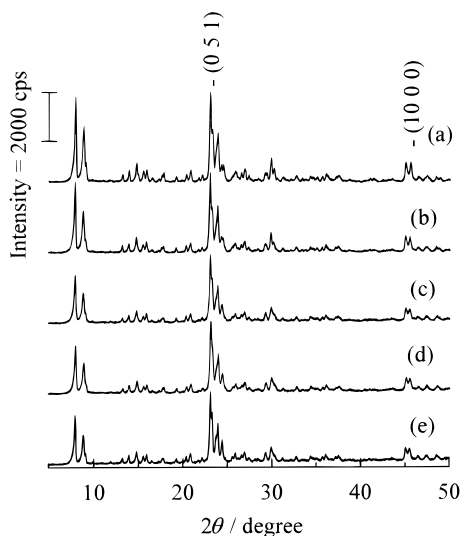


**Figure 1.** X-ray diffraction of silicalite (a) and H-ferrisilicate with 0.08 (b), 0.15 (c), 0.23 (d), and 0.40 mol kg<sup>-1</sup> (e) iron content.

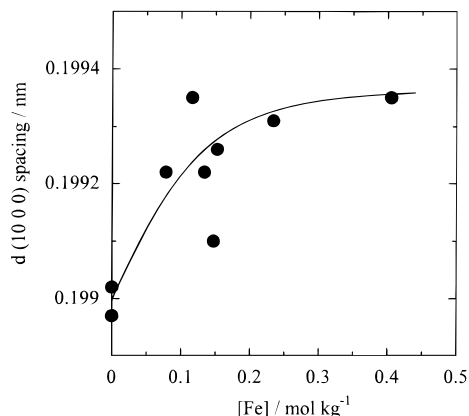
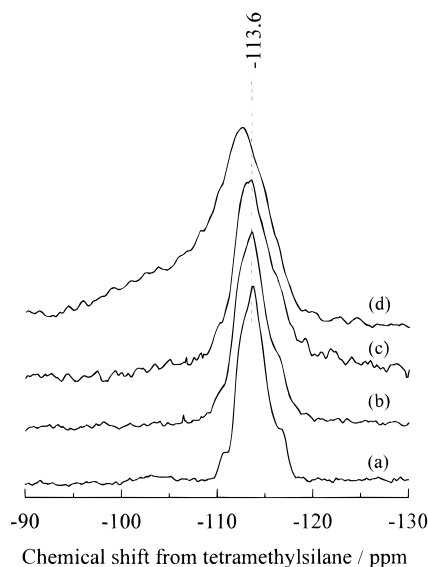


**Figure 2.** *d*-spacing of (10 0 0) plane determined from XRD.

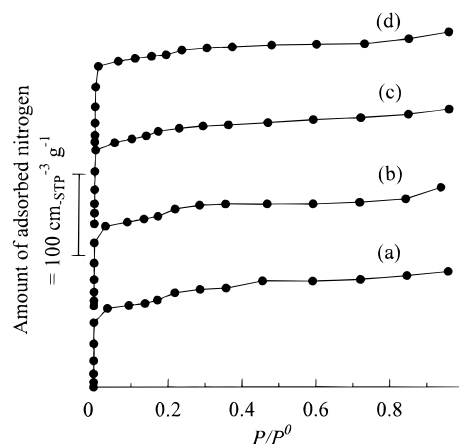
structure. It is known that the unit cell volume becomes larger when large iron atoms substitute for the silicon atoms in the crystal framework.<sup>38</sup> Figure 2 points out that the *d*-spacing increased with incorporation of 0.1–0.2 mol kg<sup>-1</sup> iron, but further increase of iron hardly increased the *d*-spacing.

Moreover, <sup>29</sup>Si NMR supports the MFI structure and the incorporation of iron into the framework. As shown in Figure 3, the Si(OSi)<sub>4</sub> peak characteristic to the MFI structure at -114 ppm was observed over the iron content range. The spectra of the samples with 0.08 (Figure 3b) and 0.15 mol kg<sup>-1</sup> iron (Figure 3c) seem to consist of the main peak at -114 ppm and a shoulder at a slightly higher magnetic field, showing the presence of Si(OF<sub>e</sub>)(OSi)<sub>3</sub> species. However, the spectrum of the sample with 0.40 mol kg<sup>-1</sup> iron (Figure 3d) was very broad and seems to contain various fractions of Si(OF<sub>e</sub>)<sub>*m*</sub>(OH)<sub>*n*</sub>-(OSi)<sub>4-*m-n*</sub>. Also ESR showed the presence of both framework and extraframework iron species on the sample with the high iron content (0.15–0.40 mol kg<sup>-1</sup>) by the resonances at *g* = 4.3 and 2.0 (data not shown).

The adsorption isotherm of nitrogen at 77 K, shown in Figure 4, on all the synthesized ferrisilicates was close to I type, showing the microporous structure, and the adsorption capacity was high enough. However, the isotherm did not have a complete plateau, suggesting the formation of macropores (greater than several tens of nanometers in diameter).<sup>39</sup> This is in agreement with the SEM showing quite small (<100 nm) crystallite size of these ferrisilicates.



**Figure 3.** <sup>29</sup>Si MAS NMR spectra of silicalite (a) and H-ferrisilicate with 0.08 (b), 0.15 (c), and 0.40 mol kg<sup>-1</sup> (d) iron.



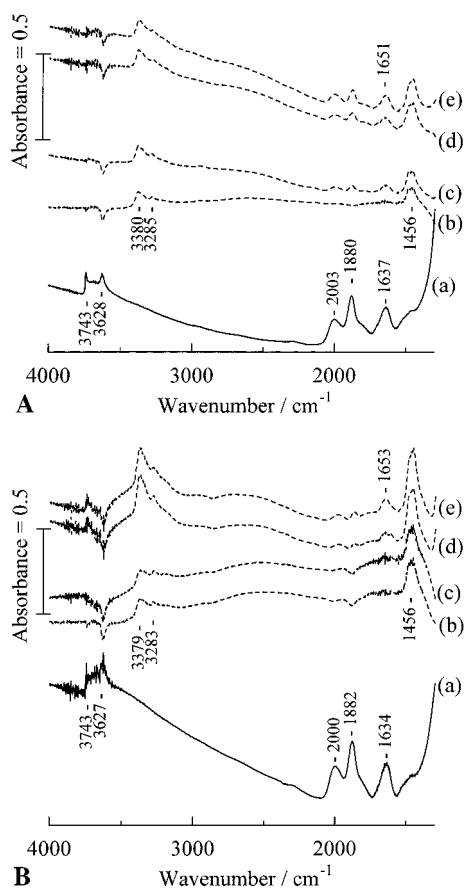
**Figure 4.** Nitrogen adsorption isotherm at 77 K on H-ferrisilicate with 0.08 (a), 0.15 (b), 0.23 (c), and 0.40 mol kg<sup>-1</sup> (d) iron.

Figure 5 shows the IR spectra of the H-ferrisilicate samples with relatively low (A) and high (B) iron contents. The spectra of both evacuated samples were similar to the reported ones, demonstrating the presence of both the terminal silanol and bridged hydroxyl group (ca. 3745 and 3630 cm<sup>-1</sup>, respectively) and skeletal vibrations (ca. 2000, 1880, and 1630 cm<sup>-1</sup>).<sup>1</sup> A qualitatively similar spectrum was observed on other samples.

**Spectrum of Adsorbed Species.** Figure 5b–d shows the differential spectra of ammonia. On both samples, N–H vibration (ca. 3380 and 3285 cm<sup>-1</sup>) and deformation bands of both ammonium cation adsorbed on Brønsted acid site (1456 cm<sup>-1</sup>) and ammonia molecule coordinated on Lewis acid site (ca. 1650 cm<sup>-1</sup>) appeared with diminishing of the acidic hydroxyl group (ca. 3630 cm<sup>-1</sup>) after the exposure to ammonia. Contact with water vapor gave almost no change in the spectrum, as shown in Figure 5e.

The spectrum of adsorbed pyridine shows that Brønsted acidity was predominant where the iron content was small, and increase of iron enhanced Lewis acidity (Figure 6).

**Temperature-Programmed Desorption.** On many zeolitic aluminosilicates<sup>15,16,27</sup> and gallosilicates,<sup>36</sup> the TPD spectrum had two peaks, namely *l*- and *h*- (low and high temperature) peaks.<sup>31</sup> On the MFI type the *l*- and *h*-peaks appeared at ca. 450 and 600 K, respectively, under the present conditions.<sup>27</sup> The *l*-peak



**Figure 5.** IR spectra of H-ferrisilicate with 0.15 (A) and 0.40 (B) mol kg<sup>-1</sup> iron evacuated at 773 K (a). Lines (b)–(e) are the differential spectra measured using (a) as the background after the exposure to 0.13 (b), 1.3 (c), and 13 kPa (d) of ammonia and evacuation, followed by the exposure to ca. 3 kPa of water vapor and evacuation (e) at 373 K.

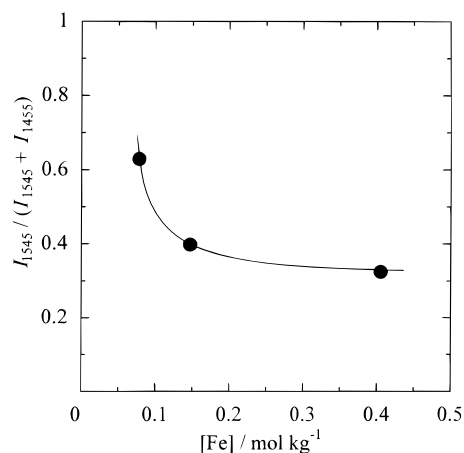


**Figure 6.** Ratio of Brønsted acid to total acid amount estimated from the IR spectrum of pyridine adsorbed at 373 K and evacuated at 573 K. The y-axis shows the ratio of intensities of pyridinium cation (1545 cm<sup>-1</sup>)/[pyridinium cation + coordinated pyridine (1455 cm<sup>-1</sup>)].

is due to the weakly held ammonia, e.g., hydrogen-bonded one, and not related to the acidic property. By contrast, the *h*-peak is ascribed to the ammonia or ammonium cation adsorbed on the acid site and must show an acidic property.<sup>15</sup> In the case of the MFI the adsorption heat of ammonia showing the *h*-peak was ca. 130 kJ mol<sup>-1</sup> within a few kilojoules per mole of distribution.<sup>27,36</sup> Water vapor treatment after the adsorption of ammonia has been known to remove the unnecessary *l*-peak on aluminosilicates.<sup>16</sup> and gallosilicates.<sup>36</sup> In addition, excess content

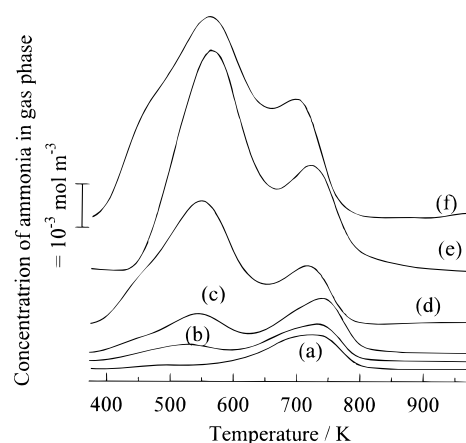


**Figure 7.** Ammonia TPD spectra of H-ferrisilicate with 0.08 (a), 0.12 (b), 0.15 (c), 0.18 (d), 0.23 (e), and 0.40 mol kg<sup>-1</sup> iron content obtained by conventional method without water vapor treatment.

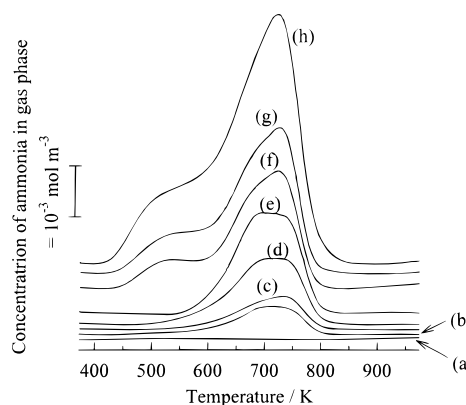


**Figure 8.** TPD spectra of silicalite (a) and H-ferrisilicate with 0.08 (b), 0.12 (c), 0.13 (d), 0.15 (e), 0.18 (f), 0.23 (g), and 0.40 mol kg<sup>-1</sup> iron content obtained by water vapor treatment method.

of aluminum or gallium or the impregnation of these metals on the MFI silicate caused the additional (*h*<sup>+</sup>-) peak at ca. 750 K, due to the exceptionally strong acid site generated by the interaction between the framework ion-exchange site and the extraframework trivalent species.<sup>32,36</sup>

However, the present ferrisilicates showed completely different behavior. Figure 7 shows the TPD spectra on the ferrisilicate measured after the adsorption of ammonia without water vapor treatment. The sample with a small amount (0.08 mol kg<sup>-1</sup>) of iron exhibited one desorption peak at relatively high temperature, ca. 700 K (Figure 7a). Increase of the iron content generated another peak at ca. 550 K, and this was predominant with more than ca. 0.2 mol kg<sup>-1</sup> iron. Figure 8 shows the spectra obtained by the water vapor treatment method. The peak of the sample with a small amount of iron at high temperature showed almost no change in the intensity and position by the water vapor treatment. On the samples with a large amount of iron, the peak at the low temperature which had been observed before the water vapor treatment was almost completely diminished, whereas the peak at the high temperature became quite large after the water vapor treatment. As a result, the position of the desorption peak became almost constant but only the peak intensity monotonically increased with increasing iron content. The change in TPD spectrum by the water vapor treatment cannot be explained by the consideration that weakly held ammonia is replaced by the water.

Detail in the change of TPD spectrum of the ferrisilicate with small amount (0.08 mol kg<sup>-1</sup>) of iron by the ammonia and water vapor treatments is shown in Figure 9. After the contact with a



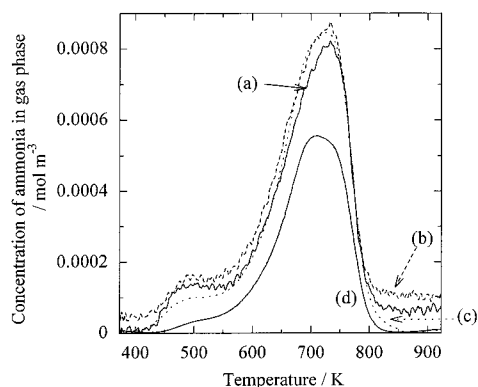


**Figure 9.** TPD spectra on H-ferrisilicate with 0.08 mol kg<sup>-1</sup> iron after exposure to a small amount (0.2 mol kg of sample<sup>-1</sup>) (a), 1.3 kPa (b), and 13 kPa (c) of ammonia followed by water vapor treatment (d).

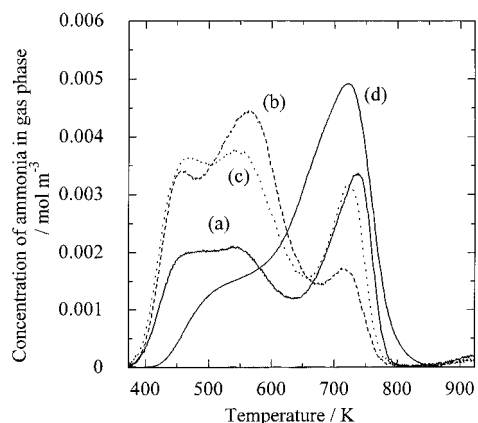


**Figure 10.** TPD spectra on H-ferrisilicate with 0.40 mol kg<sup>-1</sup> iron after exposure to a small amount (0.4 mol kg of sample<sup>-1</sup>) (a), 1.3 kPa (b), and 13 kPa (c) of ammonia followed by water vapor treatment (d).

low pressure of ammonia (Figure 9a), the desorption peak was observed at 730 K. Increase of the pressure of ammonia (Figure 9b,c) and the following water vapor treatment left the peak area, position, and shape substantially unchanged. On the other hand, the sample with a high iron content (0.40 mol kg<sup>-1</sup>) showed a complicated spectrum consisting of multiple desorption peaks at 450, 550, and 750 K after contact with low pressure of ammonia as shown in Figure 10a. Increasing the ammonia pressure suppressed the peak at the highest temperature and enhanced the intensity of the peaks at the low temperature (Figure 10b,c). The following water vapor treatment made the peak at the high temperature quite large and diminished the peaks at the low temperatures almost completely.

As a comparison, the TPD spectrum was recorded on iron oxide Fe<sub>2</sub>O<sub>3</sub> and the iron-impregnated ferrisilicate (Figure 11). The behavior of these materials was intrinsically similar to that of the ferrisilicate with high iron content. Without the water vapor treatment the desorption peak was observed at 400–500 K, and the water vapor treatment removed the peak at the low temperature and enhanced the peak at the high temperature.

The amount of ammonia adsorbed can be estimated from the peak intensity. From the conventional TPD method without the water vapor treatment, generally the adsorption amount exceeds the iron content. This is inconsistent with the stoichiometric generation of acid site by isomorphous substitution of trivalent cation into the silicate matrix. As observed on aluminosilicates, it is considered that this adsorption amount contains the ammonia adsorbed on nonacidic site, e.g., hydrogen-bonded on the ammonium ion to form an oligomer.<sup>16</sup> The

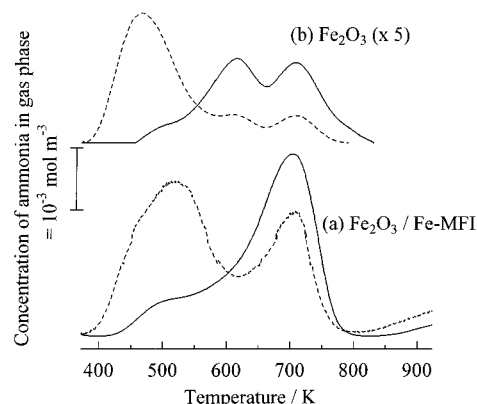


**Figure 11.** TPD spectra of iron impregnated on ferrisilicate (a) and iron oxide (b) measured by conventional (broken lines) and water vapor treatment methods (solid lines). The iron content of original ferrisilicate of the sample (a) was 0.12 mol kg<sup>-1</sup>, and the amount of iron impregnated was 1.06 mol kg<sup>-1</sup>.

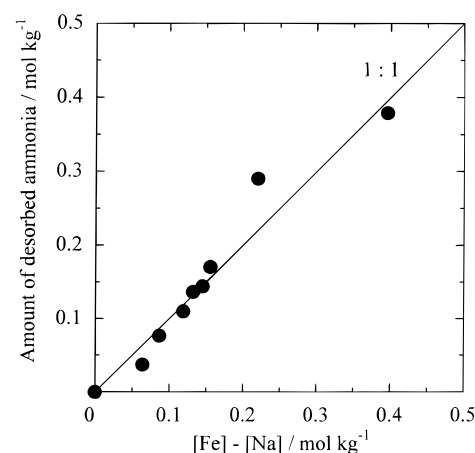


**Figure 12.** Relationship between acid amount and [Fe]–[Na] content of H-ferrisilicate determined from water vapor treatment method of ammonia TPD.

unnecessary species must be replaced by the water vapor, and the adsorption amount after the water vapor treatment is considered to show the acid amount of the ferrisilicate. The thus-determined acid amount is plotted in Figure 12. Since the samples contain a small amount of sodium, the acid amount was plotted against the [Fe]–[Na] content (close to the [Fe] content because the sodium content was low). Obviously the acid amount possessed a linear 1:1 relationship against the [Fe]–[Na].

We have proposed a curve-fitting method based on the thermodynamics to calculate the adsorption heat of ammonia and its distribution as a measure of acid strength from the area, position, and shape of the TPD spectrum.<sup>27</sup> It assumes that the desorption process is controlled by the equilibrium between the gaseous and adsorbed ammonia, but neither the diffusion nor kinetic control process. Its validity has been confirmed on various zeolites<sup>27</sup> and nonzeolitic catalysts.<sup>35</sup> Moreover, the present ferrisilicate samples have small crystallite size, as shown by the nitrogen adsorption and SEM; this is an advantage to avoid the diffusion control. Hence this analysis method was applied to the spectrum obtained by the water vapor treatment. Generally the observed spectrum was fitted well with the simulated curve, and the adsorption heat of ammonia was determined to possess within a few kilojoules per mole of distribution, as those on various aluminosilicates. As shown in Figure 13, the adsorption heat 150–180 kJ mol<sup>-1</sup> was quite a bit higher than those on the MFI-type aluminosilicate (ZSM5)<sup>27</sup>

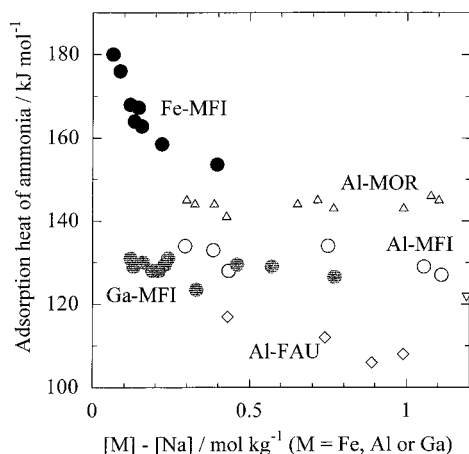


**Figure 13.** Acid strength (adsorption heat of ammonia) of MFI-type ferrisilicate determined from water vapor treatment method (●). As a comparison, the adsorption heats of the MFI-type aluminosilicates (○) and gallosilicates (gray circle), and MOR (△), BEA (▽), and FAU-type (◇) aluminosilicates are overlapped.

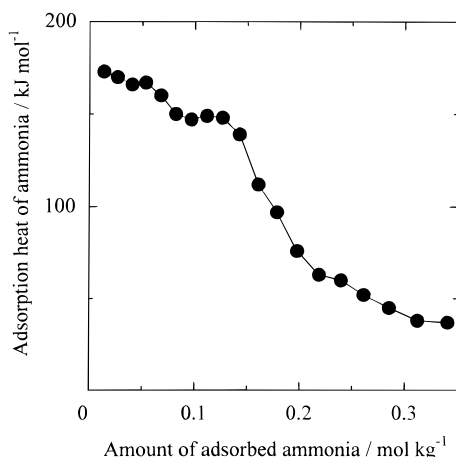


**Figure 14.** Differential heat of ammonia adsorption measured by microcalorimetry on H-ferrisilicate with 0.15 mol kg<sup>-1</sup> iron.

and gallosilicates<sup>36</sup> (both ca. 130 kJ mol<sup>-1</sup>), and exceeded the adsorption heat of MOR-type aluminosilicate (145 kJ mol<sup>-1</sup>),<sup>27</sup> which is believed to have the strongest acidity among aluminosilicate zeolites.

**Microcalorimetry.** Figure 14 shows the differential adsorption heat determined from the microcalorimetry on the ferrisilicate with 0.15 mol kg<sup>-1</sup> iron. The initial adsorption heat was quite high, ca. 175 kJ mol<sup>-1</sup>. The heat decreased at 0.07 mol kg<sup>-1</sup> adsorption amount into 150 kJ mol<sup>-1</sup> and again at 0.15 mol kg<sup>-1</sup> into <100 kJ mol<sup>-1</sup>. Probably the ammonia with the low adsorption heat appearing at >0.15 mol kg<sup>-1</sup> amount is adsorbed on the nonacidic site, because the amount of ammonia is larger than that of iron. Therefore this sample is concluded to have the two types of acid sites with 0.15 mol kg<sup>-1</sup> amount and 150 and 175 kJ mol<sup>-1</sup> adsorption heat. As shown in Figure 8e, the TPD spectrum of this sample obtained by the water vapor treatment method seems to have two overlapping peaks at ca. 670 and 730 K. The determined acid amount was ca. 0.15 mol kg<sup>-1</sup> (Figure 12), and the averaged adsorption was calculated to be ca. 165 kJ mol<sup>-1</sup> (Figure 13). Thus acidic property determined from the TPD with the water vapor treatment method is in good agreement with the calorimetric results.

**Catalytic Activity.** Catalytic cracking of *n*-octane was performed by a pulse method in differential conditions, and the activity was plotted against the [Fe]–[Na] content as shown in

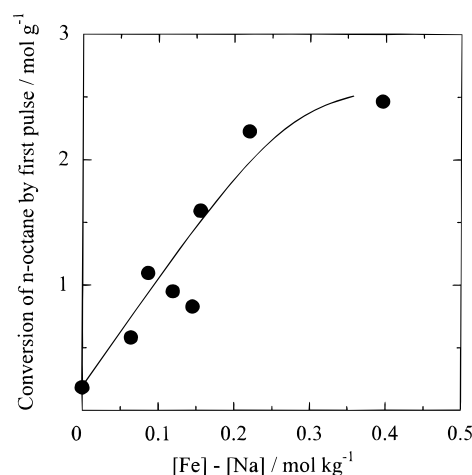


**Figure 15.** Catalytic activity for cracking of *n*-octane at 673 K on MFI-type ferrisilicate. The activity is shown by the amount of the converted *n*-octane by the first pulse of *n*-octane (1 mm<sup>3</sup>).

Figure 15. Even on silicalite a low activity was observed. The activity monotonically increased with increasing iron content over 0–0.4 mol kg<sup>-1</sup>, and this was similar to the increase in the acid amount shown in Figure 12. In contrast, almost no activity for the cracking of isooctane (2,2,4-trimethylpentane) was observed (data not shown). This confirms that the reaction of *n*-octane proceeded in the micropore which possessed the reactant-shape selectivity.

## Discussion

XRD, NMR, ESR, and IR spectroscopies, and nitrogen isotherm demonstrated that all the samples had the well-crystallized MFI structure. However, XRD showed that, at iron content higher than ca. 0.2 mol kg<sup>-1</sup>, a considerable amount of iron existed as the extraframework species, and NMR supported this conclusion because multiple kinds of iron species were suggested by the broad spectrum in the high iron content region. The ESR also pointed out the presence of both the framework and extraframework species.

The TPD spectra of samples containing a low amount of iron (<0.15 mol kg<sup>-1</sup>), where the isomorphous substitution of iron occurred as above, were simple. The spectrum was unchanged by changing the pressure of ammonia and the water vapor treatment, suggesting a stable acidic species. Bordiga et al. reported that framework iron species in ferrisilicate with 1.71 wt % (ca. 0.3 mol kg<sup>-1</sup>) iron was so stable that the reduction peak appeared at ca. 950 K in the TPR (temperature-programmed reduction) spectrum.<sup>40</sup> The number of acid sites in the present study agreed with the number of iron atoms. We here conclude that the iron atom isomorphously substituted in the MFI framework generates the stable acid site with a strength of 150–180 kJ mol<sup>-1</sup> ammonia adsorption heat. It is noteworthy that both Brønsted and Lewis acid sites exist in the ferrisilicate as shown by the IR spectrum of adsorbed pyridine, and this was different from the cases of aluminosilicates<sup>27</sup> and gallosilicates<sup>36</sup> where Brønsted acidity was predominant.

On the other hand, the behavior of ferrisilicate in the high iron content region (>0.2 mol kg<sup>-1</sup>) was complicated. The large peak at the high temperature in the TPD spectrum was observed after the introduction of small amount of ammonia (Figure 10a). However, the adsorption heat of a fraction of acid site became weak (Figure 10b,c) after contact with high pressure of ammonia. The weakened adsorption heat was recovered by the contact with water vapor (Figure 10d). These findings point out

that the intrinsic acidity of this sample is strong, but the high pressure of ammonia changes the nature of acid site. The water vapor treatment is considered to have a role to recover this changed nature. The adsorption heat of ammonia measured by microcalorimetry was similar to the recovered one observed by the water vapor treatment method, probably because the calorimetric measurements were carried out under quite low pressure of ammonia.

On the aluminosilicates, the ammonia simply neutralizes the acid site, and the water vapor replaces the ammonia weakly held on nonacidic site.<sup>16</sup> The water vapor treatment does not affect the nature of the acid site itself in these cases. However, diminishing the strong adsorption site on the ferrisilicate by contact with high pressure of ammonia and its recovery by contact with water vapor suggest that the chemical nature of the solid surface was substantially changed by these treatments. This was also observed on the iron oxide and the iron-loaded ferrisilicate.

It is noteworthy that even in the high iron content region the 1:1 stoichiometry seems to exist between the iron and adsorbed ammonia as shown in Figure 12. This points out that the iron species formed at the high content has high dispersion. It is concluded that highly dispersed iron oxide species on the silicate, or possibly partly distorted framework trivalent atom as proposed in the case of MFI aluminosilicate,<sup>26</sup> should possess the specific chemical nature to show strong acidity after evacuation but weak acidity under high pressure of ammonia.

Unfortunately the IR spectrum of adsorbed ammonia did not clarify the reason for these behaviors, because only the presence of ammonium cation adsorbed on Brønsted acid site and ammonia molecule coordinated on Lewis acid site were shown similar to many usual solid acids. The reason for these complicated changes is the subject of the next study. However, we emphasize that the changeable nature seems substantially due to the nature of bulky iron oxide, but not ascribed to the isomorphously substituted iron.

In the application to catalyst, such an extraframework (or partly distorted) iron species may play an important role, as demonstrated by the fact that the activity for cracking of hexane monotonically increased with increasing iron content and increasing total acid amount (Figure 15). However, at least on the chemistry of generation of acidity, it should be important that the isomorphously substituted iron generates the stronger acidity than that by aluminum. This is in good agreement with the high activity of the ferrisilicate for such a difficult reaction as Friedel–Crafts alkylation.<sup>11</sup>

The strong acidity due to the framework iron atom is quite different from the conventional explanation that the ferrisilicate has weaker acidity than the aluminosilicate analogue. The conventional interpretation stands on three major pieces of evidence: (1) the ammonia TPD shows a desorption peak at a low temperature;<sup>1</sup> (2) the shift of OH band in the IR spectrum by the adsorption of probe (e.g., nitrogen) is small;<sup>3</sup> (3) the catalytic activity for alkane cracking is low. On the first point, we have shown that the conventional method of ammonia TPD changes the nature of a fraction of iron with excess ammonia, and this disturbs the interpretation. The present calorimetric measurements and change in the TPD spectrum with varying the amount of adsorbed ammonia indicate that with a small amount of ammonia the iron species shows its intrinsic nature. On the second and third points, we can point out that the spectroscopic and catalytic methods are not the absolute measurements of acid strength but a method using typical base can determine the thermodynamic parameter. Not only the acid–

base interaction but also such an interaction as physical adsorption and dipole interaction may occur between the silicate and such a probe as nitrogen, carbon monoxide, benzene, and small alkene because these probes are not a typical base, especially at the low temperature usually utilized for the IR technique. Finally, we point out that all of these studies stand on a limited number of experimental points. For example, the first paper on the ammonia TPD and stretching vibration of OH group used the ferrisilicate with 98 of the Si/Fe<sub>2</sub> ratio,<sup>1</sup> namely 0.33 mol kg<sup>-1</sup> iron content. The IR study also used the sample with 50 of the Si/Fe ratio, 0.32 mol kg<sup>-1</sup> iron content.<sup>3</sup> From the present results it is probable that the acidic nature at such a high iron content was affected by the extraframework species of iron. By contrast, our conclusion stands on the systematic experiments.

Even on the aluminosilicate MFI, we have found by careful measurements of ammonia TPD that the extraframework species of aluminum induced quite strong acidity.<sup>32</sup> The ratio of number of this type of acid site to aluminum atom was almost 1:2, suggesting that the interaction between the framework and extraframework aluminum atoms (possibly Brønsted–Lewis pair) generated this acid site. It is presumed that the strong acid site observed on the ferrisilicate is not due to this type of interaction because the number of acid sites and iron atoms was almost same. One iron atom should generate independently one acid site.

## Conclusions

1. The number of acid sites on H-ferrisilicate with MFI structure approximately agreed with the number of the iron atoms in the range of iron content 0–0.4 mol kg<sup>-1</sup>. This confirms the stoichiometric generation of one acid site by the substitution of one iron atom.
2. The acid strength (adsorption heat of ammonia) due to the framework iron was > 150 kJ mol<sup>-1</sup>, and quite a bit higher than aluminosilicate analogues.
3. Weak acidity appeared when extraframework iron (or partly distorted species) contacted with a high pressure of ammonia. This behavior is substantially due to the nature of iron oxide, but not the isomorphously substituted species.

**Acknowledgment.** The authors thank Dr. Tatsuya Takeguchi, Department of Energy and Hydrocarbon Chemistry, Graduate School of Engineering, Kyoto University, for the NMR measurements and Dr. Tomoya Inoue and Mr. Tamotsu Yoneyama, Asahi Chemical Co., for the ESR measurements. This study was partly supported by a Grant-in-Aid for Scientific Research from the Ministry of Education, Science, Sports and Culture, Japan (No. 06555243 and 11650809).

## References and Notes

- (1) Chu, C. T. W.; Chang, C. D. *J. Phys. Chem.* **1985**, *89*, 1569.
- (2) Ratnasamy, P.; Kumar, R. *Catal. Today* **1991**, *9*, 329.
- (3) Zecchina, A.; Geobaldo, F.; Lamberti, C.; Bordiga, S.; Palomino, G. T.; Areán, C. O. *Catal. Lett.* **1996**, *42*, 25.
- (4) Kustov, L. M.; Kazanski, V. B.; Ratnasamy, P. *Zeolites* **1987**, *7*, 79.
- (5) Zahradník, R.; Hobza, P.; Wichterlová, B.; Čejka, J. *Collect. Czech. Chem. Commun.* **1993**, *58*, 2474.
- (6) Vetrivel, R.; Pal, S.; Krishnan, S. *J. Mol. Catal.* **1991**, *66*, 385.
- (7) Chatterjee, A.; Chandra, A. K. *J. Mol. Catal., A: Chem.* **1997**, *119*, 51.
- (8) Oumi, Y.; Yamada, M.; Kanougi, T.; Kubo, M.; Stirling, A.; Vetrivel, R.; Broclawik, E.; Miyamoto, A. *Catal. Lett.* **1997**, *45*, 21.
- (9) Chatterjee, A.; Iwasaki, T.; Ebina, T.; Miyamoto, A. *Micro. Mesoporous Mater.* **1998**, *21*, 421.

- (10) Parrillo, D. J.; Lee, C.; Gorte, R. J.; White, D.; Farneth, W. E. *J. Phys. Chem.* **1995**, *99*, 8745.
- (11) Choudhary, V. R.; Jana, S. K.; Kiran, B. P. *Catal. Lett.* **1999**, *59*, 217.
- (12) Onaka, M.; Hosokawa, Y.; Higuchi, K.; Izumi, Y. *Tetrahedron Lett.* **1993**, *34*, 1171.
- (13) Hammet, L. P.; Deyrup, A. J. *J. Am. Chem. Soc.* **1932**, *54*, 2721.
- (14) Jentoft, F. C.; Gates, B. C. *Top. Catal.* **1997**, *4*, 1.
- (15) Niwa, M.; Iwamoto, M.; Segawa, K. *Bull. Chem. Soc. Jpn.* **1986**, *59*, 3735.
- (16) Igi, H.; Katada, N.; Niwa, M. In *Proceedings of the Twelfth International Zeolites Conference*; Tracy, M. M. J., Marcus, B. K., Bisher, M. E., Higgins, J. B., Eds.; Materials Research Society: Warrendale, 1999; Vol. 4, p 2643.
- (17) Niwa, M.; Katada, N.; Sawa, M.; Murakami, Y. *J. Phys. Chem.* **1995**, *99*, 8812.
- (18) Kotasthane, A. N.; Shiralkar, V. P.; Hegde, S. G.; Kulkarni, S. B. *Zeolites* **1986**, *6*, 253.
- (19) Vorbeck, G.; Richter, M.; Fricke, R.; Parltz, B.; Schreier, E.; Szulzewsky, K.; Zibrowius, B. *Stud. Surf. Sci. Catal.* **1991**, *65*, 631.
- (20) Berndt, H.; Martin, A.; Kosslick, H.; Lücke, B. *Microporous Mater.* **1994**, *2*, 197.
- (21) El-Malki, E.-M.; van Santen, R. A.; Sachtler, W. M. H. *J. Phys. Chem. B* **1999**, *103*, 4611.
- (22) Brabec, L.; Jeschke, M.; Klik, R.; Nováková, J.; Kubelková, L.; Meusinger, J. *Appl. Catal., A: Gen.* **1998**, *170*, 105.
- (23) Gorte, R. J. *Catal. Lett.* **1999**, *62*, 1.
- (24) In ref 23 Gorte wrote that the readsorption of ammonia is due to the microporous structure of zeolite, but this is a misunderstanding. The readsorption of ammonia is due to the equilibrium between the gaseous and adsorbed ammonia, and it should be understood that the equilibrium exists during the TPD measurements because of the low activation barrier and high adsorption heat with respect to the desorption of ammonia, but it is not related to the porous structure.
- (25) Bagnasco, G. J. *Catal.* **1996**, *159*, 249.
- (26) Woolery, G. L.; Kuehl, G. H.; Timken, H. C.; Chester, A. W.; Vartuli, J. C. *Zeolites* **1997**, *19*, 288.
- (27) Katada, N.; Igi, H.; Kim, J.-H.; Niwa, M. *J. Phys. Chem. B* **1997**, *101*, 5969.
- (28) Karge, H. G.; Dondur, V. *J. Phys. Chem.* **1990**, *94*, 765.
- (29) Masuda, T.; Fujitaka, Y.; Ikeda, S.; Matsushita, S.; Hashimoto, K. *Appl. Catal., A: Chem.* **1997**, *162*, 29.
- (30) Katada, N.; Iijima, S.; Igi, H.; Niwa, M. *Stud. Surf. Sci. Catal.* **1996**, *105*, 1227.
- (31) Niwa, M.; Katada, N. *Catal. Surveys Jpn.* **1997**, *1*, 215.
- (32) Kunieda, T.; Katada, N.; Niwa, M. In *Proceedings of the Twelfth International Zeolites Conference*; Tracy, M. M. J., Marcus, B. K., Bisher, M. E., Higgins, J. B., Eds.; Materials Research Society: Warrendale, 1999; Vol. 4, p 2549.
- (33) Kim, J.-H.; Tanabe, M.; Niwa, M. *Microporous Mater.* **1997**, *10*, 85.
- (34) Okumura, K.; Nishigaki, K.; Niwa, M. *Chem. Lett.* **1998**, 577.
- (35) Naito, N.; Katada, N.; Niwa, M. *J. Phys. Chem. B* **1999**, *103*, 7206.
- (36) Miyamoto, T.; Katada, N.; Kim, J.-H.; Niwa, M. *J. Phys. Chem. B* **1998**, *102*, 6738.
- (37) Tsutsumi, K.; Nishiyama, K. *Thermochim. Acta* **1989**, *143*, 299.
- (38) Awate, S. V.; Joshi, P. N.; Shiralkar, V. P.; Kotasthane, A. N. *J. Inclusion Phenom. Mol. Recognit. Chem.* **1992**, *13*, 207.
- (39) Bond, G. C. In *Heterogeneous Catalysis: Principles and Applications*, 2nd ed.; Oxford University Press: Oxford, 1987; p 12.
- (40) Bordiga, A.; Buzzoni, R.; Geobaldo, F.; Lamberti, C.; Giamello, E.; Zecchina, A.; Leofanti, G.; Petrini, G.; Tozzola, G.; Vlaic, G. *J. Catal.* **1996**, *158*, 486.